Journal of Ovonic Research Vol. 10, No. 4, July - August 2014, p. 115 - 125

STUDIES ON JET NEBULISER PYROLYSED INDIUM OXIDE THIN FILMS

S. MARIKKANNU[a], M. KASHIF[b], A. AYESHAMARIAM[c], N.SETHUPATHI[d]
V. S. VIDHYA[e], S. PIRAMAN[f*], M. JAYACHANDRAN[g]

[a]*Department of Physics, Arumugam Pillai Seethai Ammal College, Tiruppattur, 630 211, India*
[b]*Nano Biochip Research Group, Institute of Nano Electronic Engineering (INEE), Universiti Malaysia Perlis (UniMAP), 01000 Kangar, Perlis, Malaysia*
[c]*Department of Physics, Khadir Mohideen College, Adirampattinam, 614 701, India*
[d]*Department of Physics, Arignar Anna Government Arts College, Namakkal 637 002, India*
[e]*Department of Chemistry, Chendhuran College of Engineering and Technology, Pudukottai, 622 507, India*
[f*]*Sustainable energy and Smart materials research Lab, Department of Nanoscience and Technology , Alagappa University, Karaikudi 630 002, India*
[g]*Electro Chemical Material Science Division, CSIR, Central Electro Chemical research Institute, Karaikudi, 630 006, India*

In this work, by using Jet nebulizer technique Indium oxide thin films on the glass substrates was deposited, and it was annealed for different substrate temperatures 350º, 375º, 400º, 425º, and 450˚C. Different techniques such as X-ray diffractometer, ultraviolet-visible-near infrared (UV-vis-NIR), and Scanning electron Microscopy techniques have been used for the characterization of indium oxide (In_2O_3) nanoparticles. It was found that the as-prepared In_2O_3 powder is a pure single phase and is stable up to 350º C. The size of the particles is in the range of greater than 23 nm was determined by using Scherrer equation. The band gap was found to vary linearly with the annealing temperature. The optical transmittance was obtained nearly equal to 84%.

(Received May 9, 2014; Accepted July 18, 2014));

Keywords: JET nebulizer, UV-Vis spectroscopy, SEM, thin film and Indium oxide

1. Introduction

Transparent Conducting Oxide (TCO) films are used in active and passive form in many applications, since they are found electrically conductive and optically transparent. Among the many TCO materials, Indium Oxide (In_2O_3) is physically stable and chemically inert, as a transparent conductor. Further, it exhibits similar characteristics to SnO_2 and is superior for applications in several aspects. Hence, always there is a renewed interest in process development of In_2O_3 thin films for optical and electronic applications.

Usually, In_2O_3 crystallizes into a cubic bixtype structure and has a melting point temperature of 1910˚C. It exhibits a direct band gap between 3.55 and 3.75 eV and are highly conductive, which is an unusual property for wide band gap material.

In In_2O_3, electron concentration range is observed in the range from 10^{17} to 10^{20} cm^{-3} and its mobility is widely varying between 10 and 110 cm/Vs resulting in a resistivity between 0.1 and 10^{-3} Ω cm depending on the preparation conditions. In_2O_3 also has very interesting optical properties. It absorbs IR light waves beyond 900 nm and transmits visible light of wavelength 400

*Corresponding author: apsakthivel@yahoo.com

to 700 nm. Hence, In_2O_3 film can be used as a transparent conductive oxide material in opto-electronic devices, including light emitting diodes, photo detectors, thin film solar cells, touch panels and flat panel displays.

Because In_2O_3 is mostly developed and used in the form of thin films, it is generally characterized in terms of thin film properties, which are somewhat different from those of the bulk material. In addition, the properties of indium oxide thin films are highly dependent on the preparation conditions and parameters. So, several methods have been used to deposit these films like reactive evaporation, magnetron sputtering pulsed laser deposition, electron beam evaporation, chemical vapor deposition and chemical spray pyrolysis. Amongst these, spray pyrolysis is widely engaged because of its cost effectiveness, large area productivity and easy doping. Spray pyrolysis with novel routes are explored in this regard. Though the spray pyrolysis technique is a simple one, the preparation of device quality films is difficult because it involves many process parameters. Reproducibility is confirmed by performing characterization studies on several samples prepared under nearly the identical conditions.

Transparent conducting films of indium oxide is generally prepared by spraying an alcoholic solution usually of $InCl_3$ [1-8] and sometimes of In_2O_3 [9]. The solvent used are mainly ethanol/methanol mixed with water and rarely butyl acetate [1]. Usually a small amount of hydrochloric aid is used to stable the precursor solution. In the present study, the precursor was prepared with water mixture only to reduce the production cost of In_2O_3 films using the novel JNS pyrolysis technique here. The other process parameter such as substrate temperature has been optimized to get highly transparent and conductive indium oxide thin films.

M. Jothibas et al. reported that Indium oxide (In_2O_3) thin films are successfully deposited on microscopic glass substrate at different temperatures by spray pyrolysis technique using Indium acetate as precursor solution. The physical properties of these films are characterized by XRD, SEM, AFM, UV–visible, PL and Photo acoustic measurements. XRD analysis revealed that the films are polycrystalline in nature having cubic crystal structure with a preferred grain orientation along (222) plane. The average transmittance in the visible region is found to vary from 60% to 93% depending upon the substrate temperature. The complete vibrational analysis has been carried out and the optimized parameters are calculated using HF and DFT (LSDA, B3LYP and B3PW91) methods with 3-21G(d,p) basis set for In_2O_3. The fundamental frequencies are calculated and assigned according to the experimental frequencies [10].

The effect of Fe substitution for Co on direct current (DC) electrical and thermal conductivity and thermo power of $Ca_3(Co_{1_x}Fex)_4O_9$ (x ¼ 0, 0.05,0.08), prepared by a sol–gel process, was investigated in the temperature range from 380 down to 5K.The results indicate that the substitution of Fe for Co results in an increase in thermo power and DC electrical resistivity and substantial (14.9–20.4% at 300K) decrease in lattice thermal conductivity. Experiments also indicated that the temperature dependence of electrical resistivity ρ for heavily substituted compounds $Ca_3(Co_{1_x}Fex)_4O_9$ (x ¼ 0.08) obeyed the relation lnρ p $T^{-1/3}$ at low temperatures, T ^{o} at 55K, in agreement with Mott's two-dimensional(2D)variable range hopping model. The enhancement of thermo power and electrical resistivity was mainly ascribed to a decrease in hole carrier concentration caused by Fe substitution, while the decrease of thermal conductivity can be explained as phonon scattering caused by the impurity. The thermoelectric performance of $Ca_3Co_4O_9$ was not improved in the temperature range investigated by Fe substitution largely due to great increase in electrical resistivity after Fe substitution [11].

A. Ayeshamariam et al reported that various techniques such as differential scanning calorimetry-thermo- gravimetric analysis(DSC-TGA),Fourier transform infrared spectroscopy (FTIR),ultraviolet- visible-near infrared(UV-vis-NIR),photoluminescence (PL),> as well as electrical and sensor techniques have been used for the characterization of indium oxide (In_2O_3) nanoparticles. Here, we also provide insight regarding the optical and electrical characteristics of In_2O_3 nanostructures. The impact of highly sensitive and fast responding gas sensors using In_2O_3 nanostructures is also discussed. It is found that the as-prepared In_2O_3 powder is a pure single phase and is stable upto 800 ºC. The size of the particles is in the range of 12 nm as determined by transmission electron microscopy (TEM).The bandgap was found to vary linearly with the annealing temperature. A good sensitivity upto 400 ppm was obtained for ethanol and a mechanism is proposed [12]

In this paper, investigations in relation to the JNS pyrolysis preparation of In_2O_3 thin films on glass substrates, their structural, electrical and optical characterizations are summarized. In JNS pyrolysis technique, the process parameters highly govern the film properties. Hence, their

optimization has been done to get high quality In_2O_3 films with high electrical conductivity and transmittance.

2. Experimental conditions used in film preparation

The solution was prepared with 0.1 M of indium acetate in 100 ml of triple distilled water. For increasing the solubility of the solute few drops of concentrated hydrochloric acid was added to the solution. The mixed solutions were stirred well and heated for three hours at 60 °C. This solution was sprayed on to glass substrates heated at temperatures 350, 375, 400, 425 and 450 °C in air, so that, pinhole free and uniform In_2O_3 films of thickness about 320 - 380 nm were obtained. Initially, in order to fix the concentration and temperature for indium oxide film growth, the indium concentration was varied and the temperature of deposition was also varied against thickness build-up.

Growth of In_2O_3 Films with Precursor Concentrations and volume

Indium oxide films are prepared at a substrate temperature of 400˚C with different indium acetate concentration of 0.025 M, 0.05 M, 0.10, 0.15 M and 0.20 M. The thickness of the films measured by the Profilometer is about 0.250, 0.295, 0.370, 0.390, and 0.410 μm respectively. As the growth is small above 0.1M, further use of increased quantity of indium precursor is unwanted. Further, the volume of the precursor was varied as 1, 3, 6, 9 and 12 ml for preparing the In_2O_3 films and their resistivity values were found to be about 145, 86, 24, 36 and 65 ohm cm respectively. This best supportive result for fixing a low volume of 6 ml indium precursor for all the preparation of indium oxide films in the present JNS pyrolysis technique and the concentration of Indium acetate precursor is chosen as 0.1M.

Film Thickness Variations with Substrate Temperature

Thickness dependence of In_2O_3 films deposited at different substrate temperature was studied. The thickness value was found to be about 0.540, 0.465, 0.390, 0.345 and 0.320 μm for the IO films deposited at 350, 375, 400, 425 and 450°C respectively. The film thickness decreased with the increasing substrate temperature. This may be due to the reduction of precursor volume reacting and adhering to the substrate. The reduced mass reaching the substrate is due to the increased heat convection from the substrate, pushing the droplets away there by reducing thickness built-up with temperature. This type of thickness reduction is reported for many oxide films prepared by the chemical spray pyrolysis method [10, 11] at elevated temperatures.

Visual observation showed that IO films deposited at 350˚C are thicker but the film is foggy in nature. However, at 400˚C, the foggy nature of the film surface completely disappeared and the films became highly transparent. At higher temperatures (>450˚C) the film surface is powdery because of homogeneous nucleation.

The structure of the In_2O_3 thin films prepared by the JNS technique is characterized by x-ray diffraction analysis. These films showed polycrystalline nature for all the deposition conditions and have lattice parameters corresponding to those of cubic In_2O_3 crystal [13]. A study of In_2O_3 films deposited at different temperature conditions are presented in this section.

Substrate temperature is a crucial deposition parameter in JNS pyrolysis deposition of transparent conducting oxide films. In order to study the influence of substrate temperature on the composition and crystalline properties of In_2O_3 films, temperature was varied between 350 and 450˚C. Structural developments of In_2O_3 thin films as a function of deposition temperature are shown in Fig.1. All the In_2O_3 films prepared at different substrate temperatures showed polycrystalline nature. XRD spectra exhibited peaks with diffraction patterns correspond to the body centered cubic (bcc) structure of In_2O_3 and are indexed according to the JCPDS standards (Card No. 06-0416, space group - Ia3). Investigated indium oxide films for the 2θ scans between 20˚ and 70˚ indicated a slightly (222) preferred orientation. For the films deposited between 350˚C and 400˚C, the increase of temperature leads to an improvement in crystallinity. The film prepared at 400˚C exhibits highly intense peaks at 30.468˚, 35.353˚, 50.931˚ and 60.514˚ corresponding to the (222), (400), (440) and (622) planes respectively. Additional peaks with less intensity are also seen corresponding to the planes (411,) (413) and (611). At high temperature depositions, the peak intensity decreases and this may be due to the evaporation of the indium salt that leads to homogeneous nucleation, forming powdery surface [14, 15]. The observed 2θ and the interplanar

distance d values for the intense peaks are compared with the standard JCPDS data and are listed in Table 1.

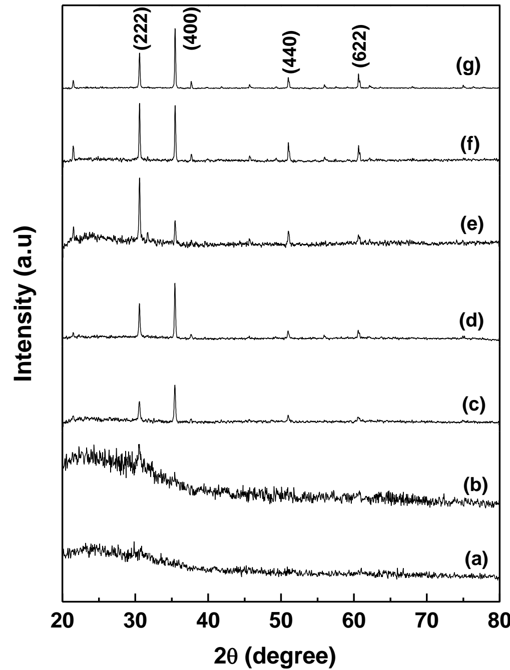

Fig.1 XRD pattern of spray deposited In_2O_3 thin films with different substrate Temperatures (a) 250 (b) 300 (c) 350 (d) 400 (e) 450 (f) 500 and (e) 550 °C

Table.1 XRD Results of Samples Deposited at (a) 350˚C (b) 375˚C (c) 400˚C (d) 425˚C (e) 450˚C

Sample	Diffraction angle 2θ		Inter planar distance d_{hkl}		hkl
	Observed (deg)	Standard (deg)	Observed (A˚)	Standard (A˚)	
(a)	30.421	30.579	2.934	2.921	222
	35.337	35.464	2.537	2.529	400
	50.910	51.035	1.792	1.788	440
	60.421	60.674	1.530	1.525	622
	30.446	30.579	2.932	2.921	222
(b)	35.343	35.464	2.537	2.529	400
	50.924	51.035	1.791	1.788	440
	60.481	60.674	1.528	1.525	622
	30.468	30.579	2.930	2.921	222
(c)	35.353	35.464	2.536	2.529	400
	50.931	51.035	1.791	1.788	440
	60.514	60.674	1.528	1.525	622
	30.432	30.579	2.934	2.921	222
(d)	35.339	35.464	2.537	2.529	400
	50.924	51.035	1.791	1.788	440
	10.445	60.674	1.530	1.525	622
	30.445	30.579	2.933	2.921	222
(e)	35.352	35.464	2.536	2.529	400
	50.926	51.035	1.791	1.788	440

From Table 1 it is observed that the interplanar distance between the various crystalline planes of the deposited In_2O_3 films are lesser or higher than the standard values. This shows that the unit cell volume is changed that in turn reveals a stress in all the films [16-18]. Due to the

presence of stress, there must be strain and these parameters are calculated from the full width at half maximum (FWHM) values of the XRD peaks. The measured parameters are listed in Table 2 for their preferentially oriented (222) plane.

Table .2 Measured Grain Size, Dislocation Density and Micro Strain of In_2O_3 Films Deposited at Different Substrate Temperature

Substrate temperature ˚C	(222) Inter plannar distanceÅ	Unit cell side (a)Å	FWHM (degree)	Grain size (D) nm	Micro strain (ε) X 10^{-3}	Dislocation density X10^{14} cm^{-2}
350	2.934	10.164	0.38	23.4	1.74	8.94
375	2.932	10.157	0.31	28.7	1.42	7.12
400	2.930	10.150	0.24	36.4	1.28	5.92
425	2.934	10.164	0.21	42.3	1.19	4.71
450	2.933	10.160	0.20	45.1	0.81	1.24

It is clear from the Table 2 that the unit cell dimension of all the In_2O_3 films is greater than the bulk value 10.11 Å. The films deposited at 400˚C shows the minimum value of 10.150 Å among the others. It is evident that grain size of the In_2O_3 films increases with the increase in substrate temperature for the (222) oriented crystallites. This trend of increase in grain size with temperature is reported already for the doped In_2O_3 films [19].

The crystals defect parameters such as microstrain and dislocation density are estimated [20] and their variations with respect to the substrate temperature are explicit from the table. The microstrain shows a decreasing trend with increasing in substrate temperature. This type of change in strain may be due to the recrystallization process observed in the polycrystalline oxide films. At high substrate temperature both the microstrain and dislocation density are minimum, which revealed the reduction in the concentration of lattice imperfections leading to highly crystallized films with preferred orientations. This type of result is suggested by other workers [21, 22] for the TCO films prepared by various chemical based and other techniques.

For an increase in temperature, the films show crystalline structure and the intensity of (222) plane increases up to 400°C. Other planes (400) and (440) with considerable intensity are also present, but their intensity is lesser than the intensity of (222) plane. Above this temperature, the preferred orientation of the film changed from (222) to (400) direction. It shows that the intensity of (222) peak is reduced or equal to that of (400). A similar change of growth pattern has also been observed for ZnO [23] and SnO_2 [24] films. Because of these peak intensity variations, the films prepared with different temperatures below and above 400°C are electrically resistive and optically less transparent due to their structural disorder [24].

Optical properties In_2O_3 films

In_2O_3 films prepared by JNS technique at various substrate temperatures between 350-450˚C under the optimized deposition conditions were studied for their optical properties. The optical transmittance curves of JNS pyrolysed indium oxide films have been obtained in the 300-900 nm spectral regions. From the measured spectral transmittance, the optical absorption co-efficient (α), optical energy gap (E_g), were calculated using the method proposed by Swanepoel [25] especially using the transmittance spectrum in the transparent and weak absorption region.

Fig. 2 depicts the optical transmittance spectra of the In_2O_3 films deposited under optimized conditions at different substrate temperatures. Films deposited at lower substrate temperature, 350˚C exhibited a slight milky appearance and the transmittance is less compared to that of the films deposited at high temperatures. The percentage of transmittance (%T) in the uv-visible region is found to increase with increasing deposition temperature. Highest transmittance value of about 88% is observed for the In_2O_3 films prepared at 400˚C. The increase in transmittance is attributed to the well adherent and the nanocrystalline nature of the films as revealed from the XRD results, which explicity showed high peak intensities due to uniform oxidation of In_2O_3 film and improvement in the lattice atomic arrangements [4]. In the case of higher substrate temperatures above 400˚C, there is a drop in transmittance due to the increased

surface irregularity and impaired crystallinity. Evaporation of mist like solute in this JNS process at high deposition temperature leads to films with less stoichiometry. The crystallinity deviation produce less intense peak as evidenced from the XRD results for the In_2O_3 films deposited higher temperatures.

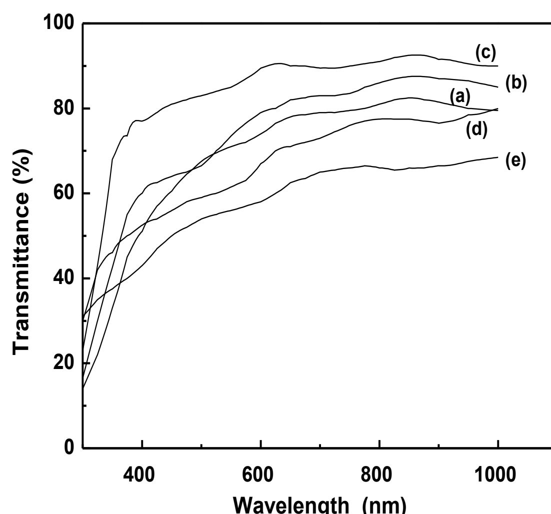

Fig 2. Optical transmittance spectra of In_2O_3 films deposited at different substrate temperatures (a) 350, (b) 400, (c) 450, (d) 500 and (e) 550°C

The recorded transmittance spectra showed wide interference waves due to the outcome of the interference of light reflected between the air/film and film/substrate interfaces. As the substrate temperature increases, the interference effects also become prominent. Further, there is a sharp fall in the transmittance curve for the film deposited at 400°C, which shows the highly crystallized and nanocrystalline nature of the films.

From the optical transmittance curves, the optical band gaps of the nanocrystalline In_2O_3 films are evaluated. The optical absorption α related to the optical band gap of the prepared films at different substrate temperature satisfies the equation

$$\alpha h\nu = A (h\nu - E_g)^{1/2} \quad (1)$$

A typical plot is presented in Fig.2. It can be observed that the plot is linear in the region of strong absorption i.e. near the fundamental absorption edge seen at the ultraviolet region. The linear intercept at the hν-axis gives the direct allowed band gap value of 3.69, 3.72, 3.92, 3.81 and 3.71eV. The values are estimated values for In_2O_3 and are in good agreement with the previously reported values [26]. Also, this high value of band gap confirms the surface smoothness and uniformity of the In_2O_3 films prepared under the optimized JNS conditions. Further, the In_2O_3 films prepared at 400˚C have a band gap of 3.92 eV with the preferred orientation along (222) plane. This is in good agreement with the observation that the band gap values of the order of 3.71 - 3.82 eV are accompanied with (222) orientation for the In_2O_3 films prepared by the thermal evaporation technique [27].

Electrical properties variation with temperature

The electrical resistivity measurements have been carried on In_2O_3 films using the conventional linear four-probe technique and the mobility and carrier concentration variations using Hall probe technique. In_2O_3 films deposited at 350, 375, 400, 425 and 450°C were characterized at room temperature. The results obtained are presented in this section.

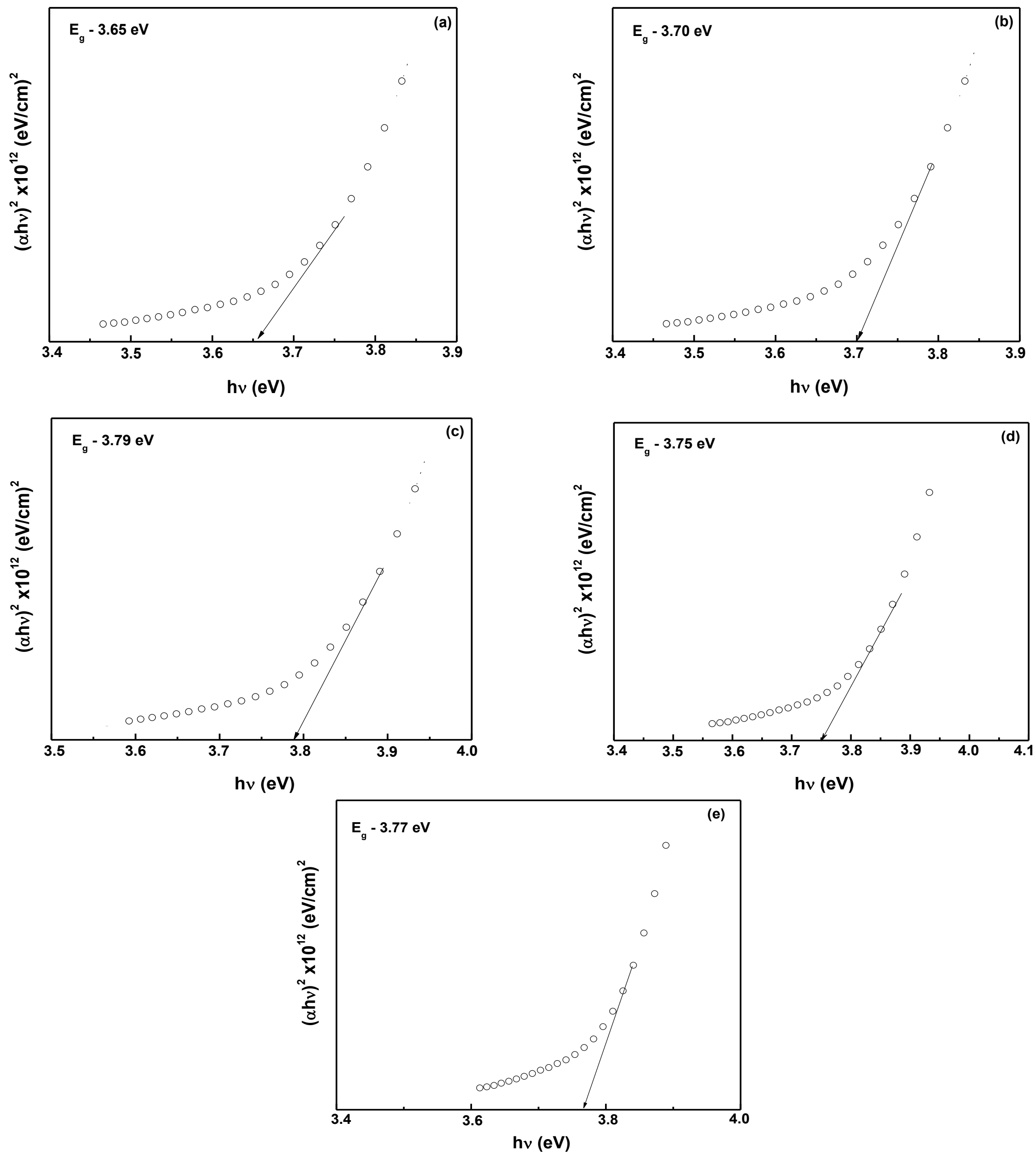

Fig. 3. $(\alpha h\gamma)^2$ vs hγ plots for In_2O_3 films deposited at different substrate temperatures (a) 350 (b) 400 (c) 450 (d) 500 and (e) 550 ^oC

The hot probe observation and the negative sign of the Hall coefficient have confirmed the n-type semiconducting nature in In_2O_3 films. The effect of deposition temperature on the resistivity, carrier concentration and Hall mobility are plotted in Fig.4. It is seen that the In_2O_3 films prepared at 400˚C have shown high carrier concentration of about 4.30 x 10^{-19} cm^{-3}, high mobility value of 13.75 cm^2/Vs and low resistivity of $1.5x10^{-2}$ ohm cm. This may be due to the degenerate nature of the IT films prepared under the JNS optimized conditions. Normally in In_2O_3 films, degenerate property is observed even below this measured value [28-30]. In addition, it is observed that the carrier concentration increases up to the deposition temperature 400˚C and then shows a decreasing trend upto 450˚C.

This decreasing trend is attributed to the observed increment of the grains and grain boundaries with increase of substrate temperature as seen from the SEM pictures shown in Fig 5. These increased grain boundaries are acting as traps for charge carriers and hence reduce the carrier concentration. In the present study of indium oxide thin films, it has been already observed

from the XRD analysis that the crystallinity decreases at high deposition temperature due to the formation of structural defects.

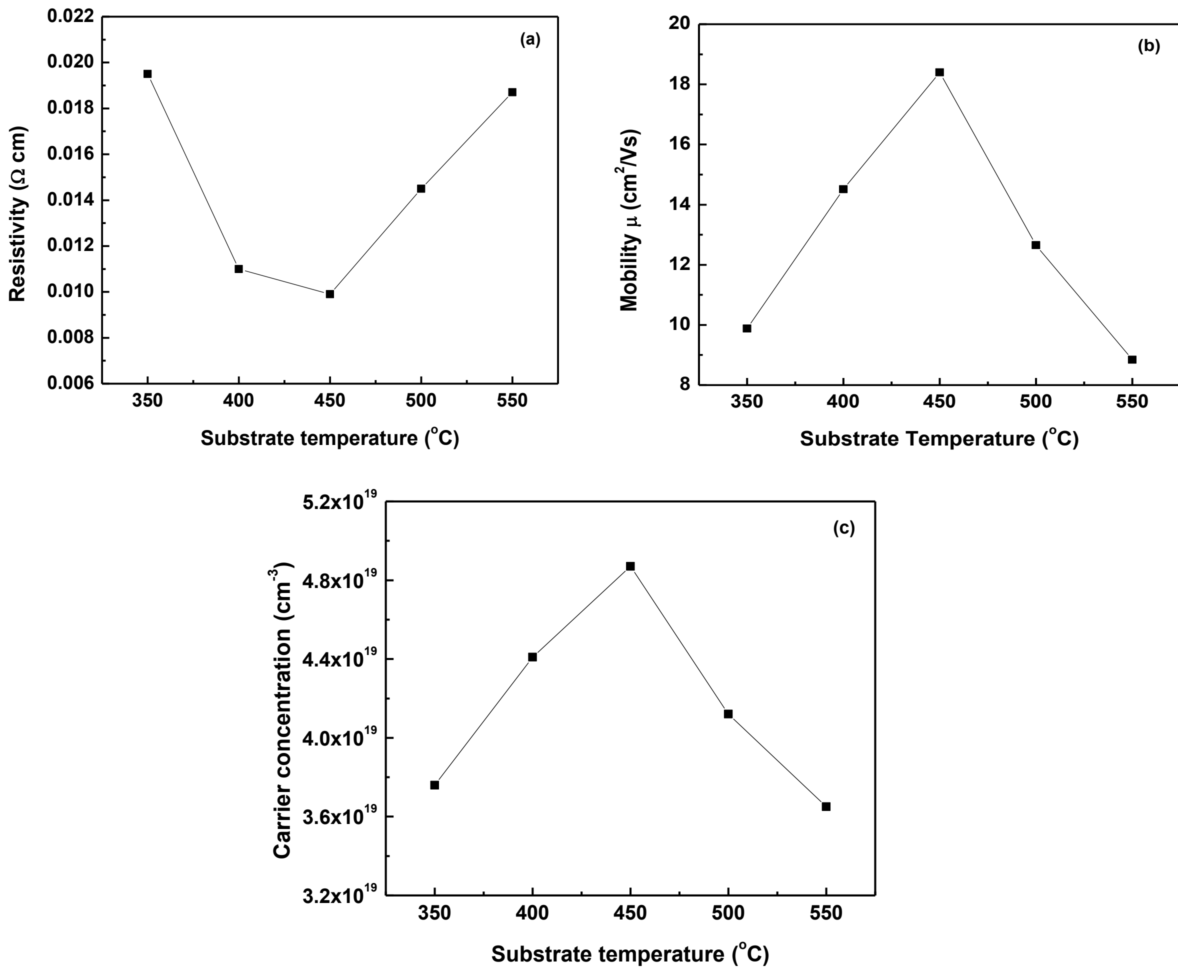

Fig 4. Variation of resistivity (a), mobility (b) and (c) carrier concentration of In_2O_3 film with substrate temperature

The Hall mobility variation is showing a similar trend as that of carrier concentration, which increases up to 400˚C and then decreases. The Hall mobility is influenced by the following defects in the oxide films: (i) a grain boundary scattering, (ii) an ionized impurity scattering, (iii) a neutral impurity scattering and (iv)scattering at other defects and dislocations [31]. However, a maximum value of 13.75 cm^2/Vs has been obtained in the present study of JNS prepared IO films, and these values are in good agreement with the reported mobility values [4, 9] for various In_2O_3 films. For the optimal deposition conditions, JNS deposited In_2O_3 films are predominantly (222) oriented for which condition of oxide materials the number of scattering centers are minimum [32] and hence these indium oxide film possesses high mobility.

The mean free path values of carriers are calculated using the relation [31],

$$l = \frac{h}{2e}\left[\frac{3n}{\pi}\right]^{\frac{1}{3}} \mu_H \tag{4}$$

where, n is the carrier concentration and μ_H is the Hall mobility.

The mean free path values of carriers calculated are in the range of 2.14-4.96 nm, which is smaller than the grain size calculated from XRD and SEM results, and hence the grain boundary scattering is very much reduced. However, there is no significant rise in carrier concentration and

this fact is revealed in the case of grain size also. Even though the grain size variations are 22 to 43 nm (from XRD studies), the carrier concentration value is nearly constant and varies only between 3.6 to 4.3 x10^{19} cm^{-3}. These results evidently confirm the dependence of electrical properties of the JNS prepared In_2O_3 films with grain size in the present study.

Microstructure study of In_2O_3 film Using SEM pictures

In_2O_3 films have been prepared by JNS technique using the optimized deposition conditions at substrate temperatures 350, 375, 400, 425, and 450˚C. The surface morphology of the JNS prepared indium oxide films are presented in Fig.5

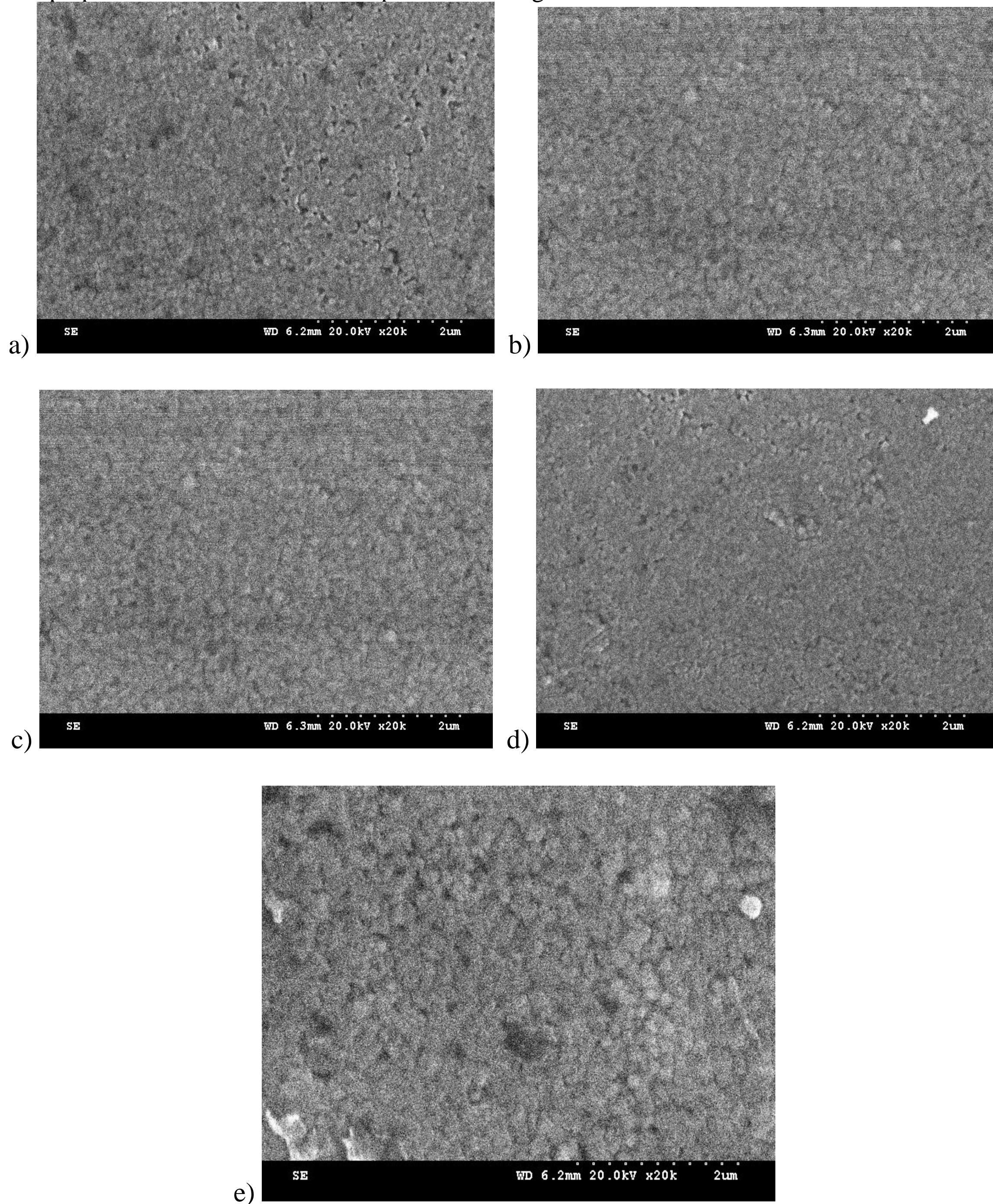

Fig 5. Variation SEM micrograph at (a) 300 (b) 350 (c) 450 (d) 500 and (e) 550ºC of In_2O_3 film.

At low deposition temperatures, the film have grain formation just initiated but with crystalline nature as seen with grainy surface and as revealed from the XRD results. The uniform and smoothest surface corresponds to the In_2O_3 films grown with a substrate temperature of 400˚C for which the XRD peak intensity is very high. At high temperature depositions, the number of nuclei formed on the surface may be somewhat decreased. This kind of film growth can be explained based on the growth mechanism proposed for the spray deposited films and their dependence on substrate temperature [33, 34]. The grain size is found increasing with deposition temperature, which are found to have agglomerated crystallites within each grain.

At lower temperatures, the solid melted and vaporized before droplets reached the substrate surface. Hence, nuclei are formed on the substrate because of the gas phase diffusion. Since the activation energy for nucleation is less at lower temperatures less than 400°C, the number and size of nuclei are small and resulted in rough surface. At 400°C deposition temperature, thermal energy is sufficient to produce more number of nuclei and they tend to combine to form bigger grains due to their high activation energy. Further, In_2O_3 films grown at higher substrate temperature at 425 and 450˚C, show clusters and irregular surface morphology

3. Conclusions

Indium oxide films have been prepared successfully using the JNS pyrolysis technique. The influences of the spray parameters like volume of the precursor solution and temperature of the substrate on the film growth, structural, and electrical properties have been studied. 0.1 M of indium acetate, 6 ml volume of this solution and a deposition temperature of 400˚C are the optimized deposition parameters to prepare In_2O_3 films in the present study.

The XRD results show the cubic structure of the In_2O_3 films with <222> as the preferred orientation along with other small peaks. The optical constants of the In_2O_3 films, (optical band gap, refractive index, extinction co-efficient) are estimated from the transmittance spectrum. Maximum transmittance of 84 % is observed for the films deposited at 400˚C. The band gap values are estimated and the extinction co-efficient values are in the order of 10^{-2}. Finally, the values of carrier concentration and mobility are found to increase when the substrate temperature is increased from 350˚C to 400˚C and then decreased. However, the resistivity decreased up to 400˚C and then increased. The high mobility value in the range of 13.75 cm^2/Vs may be due to very small mean free path values compared to the grain size value of greater than 23 nm. This lower value of mean free path has reduced the grain boundary scattering to a larger extend leading a low resistive film formation in the present study. These results are encouraging for the use of In_2O_3 films in optoelectronic device applications especially for the fabrication of low cost solar cells.

References

[1] W. Siefert, Thin Solid Films, **121**, 275 (1984).
[2] G. Korotcenkov, V. Brinzari, A. Cerneavschi, A. Cornet, J. Morante, A. Cabot, J. Arbid, Sensors and Actuator, **B84**, 37 (2002).
[3] P. K. Manoj, K.G. Gopchandran, Peter Koshy, V.K. Vaidyan, Benny Joseph, Optical Materials, **28**, 1405 (2006).
[4] J. Joseph Prince, S. Ramamurthy, B. Subramanian, C. Sanjeeviraja, M. Jayachandran, J. Crys. Growth, **240**, 142 (2002).
[5] M. Girtan, G. Folcher, Surf. and Coat. Tehnol., **172**, 242 (2003).
[6] M. Girtan, Surf. Coat. Technol., **184**, 219 (2004).
[7] C.H. Lee, C.S. Huang, Mat. Sci. Engineer., **B22**, 233 (1994).
[8] S.M. Rozati, T. Ganj, Renew. Energy, **29**, 1665 (2004).
[9] J.-H. Lee, B.O. Park, Surf. Coat. Technol., **184**, 102 (2004).
[10] M. Jothibas , C. Manoharan , S. Ramalingam, S. Dhanapandian , S. Johnson Jeyakumar M. Bououdina , Journal of Molecular Structure **1049**, 239 (2013)

[11] Yi Liu, HaijinLi, HongmeiChen , YuexiaJi et al., Journal of Physics and Chemistry of Solids **75,** 606 (2014)
[12] A. Ayeshamariam, M.Bououdina, C.Sanjeeviraja , Materials Science in Semiconductor Processing, **16**, 686 (2013)
[12] M. Krunks, E. Mellikov, Thin Solid Films, **270**, 33 (1995).
[13] A. Ayouchi, F. Martin, D. Leinen, J.R. Ramos-Barrado, J. Cryst. Growth, **247**, 497 (2003).
[14] H.L. Ma, D.H. Zhang, P. Ma, S.Z. Wid, S.Y. Li, Thin Solid Films, **263**, 105 (1995).
[15] W. DeSisto, M. Sosnowski, F. Smith, J. Deluca, R. Kershan, K. Dwight, A. World, Mater. Res. Bull., **24**, 753 (1989).
[16] J. C. Viquie, J. Spitz, J. Electrohem. Soc., **122**, 585 (1975).
[17] L.J. Meng, M.P. Santos, Appl. Surf. Sci., **120**, 243 (1997).
[18] L.J. Meng, M.P. Santos, Thin Solid Films, **303**, 151 (1997).
[19] L.J. Meng, M.P. Santos, Thin Solid Films, **322**, 56 (1998).
[20] A. El Hichou, A. Kachouane, J.L. Bubendorff, M. Addou, J. Ebothe, M. Troyon, A. Bougrine, Thin Solid Films, **458**, 263 (2004).
[21] C.K. De, N.K. Mishra, Indian J. Phys., **A71**, 530 (1997).
[22] A. Ashor, N. El-Kadry, M.R. Ebid, M. Farghal, A.A. Ramadan, Thin Solid Films, **279**, 242 (1996).
[23] N. El-Kadry, M.F. Ahmed, Hady K. Abdel, Thin Solid Films, **274**, 120 (1996).
[24] Joint Commission of Powder Diffraction Data Files, PCPDFWIN, Version 1.30, Card number 06-0416, Pennsylvania (1997).
[25] M. Suchea, G. Kiriakidis, Proc. 19th Panhellenic. Con. Sol. State Mat. Sci., (2003) 389.
[26] M. Suchea, G. Kiriakidis, CAS Proc. International Semiconductor Conference, IEEE, Vol. II, 345 (2004).
[27] Swanepoel, J. Phys. E: Sci. Instrum., **16**, 1214 (1983).
[28] M. Girtan, G.I Rusu, G.G. Rusu, Mat. Sci. Eng., B **76**, 156 (2000).
[29] A.S. Ryzhikov, R.B. Vasiliev, M.N. Rumyantseva, Mat. Sci. Eng., B **96**, 268 (2002).
[30] R.L. Weiher, R.P. Lay, J. Appl. Phys., **33**, 2834 (1962).
[31] S. Noguchi, Sakata, J. Phys. D, **13**, 1129 (1980).
[32] V. Vasu, A. Subramanyam, Thin Solid Films, **193-194**, 696 (1990).
[33] G. Sanon, R. Rup, A. Mansingh, Thin Solid Films, **190**, 287 (1990).
[34] M.G. Takawala Chitra Agashe, V.G. Bhide, J. Appl. Phys., **70**, 7382 (1991).
[35] J.C. Manifacier, L. Szepessay, J.F. Bresse, M. Perotin, R. Stuck, Mater. Res. Bull., **14**, 163 (1979).